Region 2
UNIVERSITY TRANSPORTATION RESEARCH CENTER

OPENING-MODE CRACKING IN ASPHALT PAVEMENTS: CRACK INITIATION AND SATURATION

Dr. Huiming Yin
Columbia University
Department of Civil Engineering and Engineering Mechanics
500 West 120th Street, New York, NY 10027, USA
yin@civil.columbia.edu

December 2009

Disclaimer

The contents of this report reflect the views of the authors, who are responsible for the facts and the accuracy of the information presented herein. The contents do not necessarily reflect the official views or policies of the UTRC or the Federal Highway Administration. This report does not constitute a standard, specification or regulation. This document is disseminated under the sponsorship of the Department of Transportation, University Transportation Centers Program, in the interest of information exchange. The U.S. Government assumes no liability for the contents or use thereof.

TECHNICAL REPORT STANDARD TITLE PAGE

1. Report No.	2.Government Accession No.	3. Recipient's Catalog No.
4. Title and Subtitle **OPENING-MODE CRACKING IN ASPHALT PAVEMENTS: CRACK INITIATION AND SATURATION**		5. Report Date December 2009 6. Performing Organization Code
7. Author(s) Dr. Huiming Yin		8. Performing Organization Report No.
9. Performing Organization Name and Address Columbia University Department of Civil Engineering and Engineering Mechanics 500 West 120th Street, New York, NY 10027, USA		10. Work Unit No. 11. Contract or Grant No. 49111-08-20
12. Sponsoring Agency Name and Address University Transportation Research Center City College of New York New York, NY 10031		13. Type of Report and Period Covered 14. Sponsoring Agency Code

15. Supplementary Notes

16. Abstract

This paper investigates the crack initiation and saturation for opening-mode cracking. Using elastic governing equations and a weak form stress boundary condition, we derive an explicit solution of elastic fields in the surface course and obtain the energy release rate, so that opening-mode cracking initiation can be determined by fracture energy criterion. Interestingly, the longitudinal stress between such cracks along the surface undergoes a transition from tensile to compressive with increasing applied tensile loading, which implies crack saturation. Opening-mode cracking in asphalt pavements is studied and a two-dimensional closed-form elastic solution of one section from the periodic crack pattern is derived. Using the fracture energy criterion, the proposed model predicts the OMC initiation and saturation. For an intact asphalt pavement, there exists a threshold of mismatch deformation to induce the first OMC. The stiffer the interface, the higher the threshold mismatch deformation. Once the first crack forms, the crack spacing rapidly decreases to a certain value. Therefore, multiple OMCs may simultaneously form. The stiffer the interface, the lower the crack spacing. When crack spacing approaches a certain value, the driven force to produce a new OMC will be significantly high. An asphalt pavement with a stiff interface has a narrow crack spacing range. Given asphalt material properties and loading condition, there exists a critical thickness for the asphalt overlay, below which no OMC can initiate. Therefore, a thinner asphalt overlay may produce better performance for OMCs. Because asphalt materials exhibit viscoelastic behavior, the present elastic formulation may overly predict the OMC crack density. Future work to quantitatively evaluate the effect of the assumptions and release those assumptions is underway.

17. Key Words	18. Distribution Statement
Opening-Mode Cracking, Crack initiation and Saturation, Fracture Toughness, Elastic Analysis, Asphalt Pavement	

19. Security Classif (of this report)	20. Security Classif. (of this page)	21. No of Pages	22. Price
Unclassified	Unclassified	25	

Form DOT F 1700.7 (8-69)

Opening-Mode Cracking in Asphalt Pavements: Crack Initiation and Saturation

H.M. Yin*

** Columbia University*
Department of Civil Engineering and Engineering Mechanics
500 West 120th Street, New York, NY 10027, USA
yin@civil.columbia.edu

ABSTRACT. *Opening-mode cracking has been commonly found in asphalt pavements and other layered materials with nearly uniform crack spacing. Due to the deformation mismatches between surface overlay and base layer of pavements, longitudinal tensile stress is induced in the surface course. When it reaches a certain level, transverse cracks will initiate at the surface to release the energy stored in the asphalt materials. When crack spacing reduces to a certain value, crack density is saturated and no new crack forms. This paper investigates the crack initiation and saturation for opening-mode cracking. Using elastic governing equations and a weak form stress boundary condition, we derive an explicit solution of elastic fields in the surface course and obtain the energy release rate, so that opening-mode cracking initiation can be determined by fracture energy criterion. Interestingly, the longitudinal stress between such cracks along the surface undergoes a transition from tensile to compressive with increasing applied tensile loading, which implies crack saturation. This explicit formulation is applicable to pavement structure design and opening-mode cracking analysis of asphalt pavements. If a loading condition is fixed, there exists a critical thickness of the surface overlay, below which no crack forms. Parametric analyses of opening-mode cracking are conducted considering the material stiffness, fracture toughness, interface conditions, and loading conditions. The viscoelastic effect of asphalt materials on the crack development is also discussed.*

KEYWORDS: *Opening-Mode Cracking, Crack Initiation and Saturation, Fracture Toughness, Elastic Analysis, Asphalt Pavements.*

1. Introduction

As a major form of distress in asphalt pavements and the main criterion for pavement rehabilitation, cracking in surface course exhibits a random nature and shows in diverse patterns. Many reasons contribute to surface cracking, such as

traffic loading, climate conditions, mixture properties, aging effects, construction factors, and deformation of base and subgrade layers (Myers and Roque, 2002; Wang, et al., 2003; Huang, 2003; Yin et al., 2007; Harmelink, et al., 2008). Because each cracking mechanism may produce different cracking patterns that follow distinct failure development trends, understanding of cracking mechanisms is extremely important for a pavement management system to determine appropriate pavement treatment strategies and to predict pavement performance (Luo and Yin, 2008). Therefore high standards have been set up on accurate categorization and evaluation of pavement distresses according to surface cracking mechanisms, which are crucial to pavement inspection, preservation, and maintenance.

Opening-mode cracking (OMC) has been commonly found in layered materials. When a layered material is subjected to a tensile stress, a series of uniformly distributed mode-I cracks (Anderson, 2005) will be induced in the direction perpendicular to the tensile stress to release the strain energy stored in the material. In asphalt pavements, tensile stress in surface courses can be caused by temperature and moisture changes, subgrade swollen, freeze-thaw action, and other deformation mismatched between the surface overlay and base layer. Because the tensile stress of surface overlay typically exists in a large area of pavements, OMC in asphalt pavements is not like some random cracks caused by material variation or construction issues, but exhibits a recognizable cracking pattern over several or more pavement sections. Transverse cracks may form across or partially across the width of the pavements with nearly uniform crack spacing. Depending on the load condition and the material property, the OMC crack spacing has been observed from nearly 30 meters to 1 meter as seen in Figure 1.

(a) (b)

Figure 1. Opening mode cracking in asphalt pavements with crack spacing around (a) 1 meter and (b) 10 meters. Both photos were taken in Urbana, IL in 2006

Figure 1(a) shows the OMC pattern on the driven lane of the westbound I74 between mileage #183 and #184 in Urbana, IL in 2006. Very dense OMCs were observed with crack spacing less than 1 meter. Although this type of OMCs is not rare and has been found in some other states by the author, the actual reason for this unique crack pattern has not been completely discovered yet. As a reference, some OMCs were also found on the street just side-by-side to I74 as shown in Figure 1(b) with the crack spacing of approximately 10 meters. This type of OMC has been further classified as low temperature cracking (Yin, et al., 2007). When the pavements are subjected to an ambient temperature decrease, low temperature cracking can initiate on the overlay surface due to thermal contraction and propagate toward the interface, often with a uniform crack spacing pattern. Notice that all OMCs in Figure 1(a) completely cross the width of the driving lane, whereas some OMCs in Figure 1(b) stop in the middle of the driving lane.

The purpose of this work is not to investigate the reasons or magnitude of the tensile stress in a specific asphalt pavement, but to study the opening-mode cracks (OMCs) developing with the tensile stress in an asphalt overlay in general cases. OMC initiation and saturation will be considered and formulations for OMC development will be developed. When tensile stress reaches a certain level, transverse cracks will initiate at the surface to release the energy stored in asphalt overlay. In the field, when OMCs initiate, crack spacing can be nearly a hundred feet that depends on the geometry of pavement structures. With the increase of tensile stress, additional cracks form in the layer until that crack density is saturated and no new crack forms (Bai, et al., 2000). In asphalt pavements, the dense cracking pattern in Figure 1(a) can be considered as an example of crack saturation.

It is extremely important to know the condition of OMC initiation in pavement design and failure analysis. Especially for low temperature cracking in asphalt pavements, once the low temperature properties of the asphalt materials are known, we can determine the maximum temperature change that the pavement can sustain from the developing OMCs. Therefore, we can design appropriate asphalt materials and pavement structures consider the regional climate. Inversely, from the occurrence of OMCs, we can also calculate the tensile stress within the asphalt overlay based on the material properties and investigate the failure mechanisms and prevent the similar problem in the future construction.

Crack saturation in asphalt overlay has not been widely recognized by asphalt pavement research community. However, it provides significant information for pavement management and maintenance. Once OMCs initiate in an asphalt pavement, crack development can be fast at the beginning. When crack spacing reaches a certain level, the development speed of OMC will much slows down. Certainly, such dense crack pattern may promote the possibility for some other types of distresses such as block cracking, alligator cracking, and potholes. However, in some situations, *if all other distresses are under control, the saturated OMCs may not be a primary reason for a rush rehabilitation or reconstruction because it has lost its activeness*.

In this paper, asphalt pavements are considered as an asphalt overlay placed on a base layer through a frictional interface. A deformation mismatch between the overlay and base layer, such as contractive deformation in overlay and expansive deformation in base layer, will produce tensile stress in the asphalt overlay. In

Figure 2 (a), OMCs are periodically distributed in the asphalt overlay and stopped at the interface. The two layers are assumed to be fully bonded through a frictionally interface even during the formation of the OMCs, and thus no delamination along the interface is considered. By using the simplified boundary conditions (Yin, et al., 2005; 2007; 2008), a general solution for the elastic fields of the layer will be derived in a closed form. Given a loading condition and geometric configuration of asphalt pavements, the proposed model predicts the crack initiation and crack saturation. It is predicted that the cracking spacing typically increases with the increment of the thickness of asphalt overlay. However, a critical thickness exists, below which no fracture can initiate. Therefore, under some circumstances, *a thinner overlay may even produce better performance for OMC resistance*.

The remainder of this paper is organized as follows. Section 2 presents the general solution of the elastic boundary value problem in a periodic section between two adjacent OMCs and provides an explicit expression of the elastic fields within the asphalt overlay. Section 3 derives the energy release rate of a new crack and provides a method to predict the OMC initiation, spacing, and saturation. Section 4 provides some numerical results to interpret the proposed formulation and conducts parametric analyses about OMC development. Section 5 uses one example to demonstrate the application of the proposed model to predict the OMC initiation, development, and saturation. The factors to affect OMCs, such as viscoelastic behaviour of asphalt materials, geometry of pavement structure, and aging effect of asphalt binders, are also discussed.

2. Elastic Formulation

Consider an asphalt pavement containing an asphalt overlay (thickness h, Young's modulus E_1, Poisson's ratio v_1) resting on a base layer as illustrated in Fig. 2(a). A deformation mismatch between the overlay and base layer, such as compressive deformation in overlay and expansive deformation in base layer, will induce tensile stress in the asphalt overlay. In Figure 2 (a), OMCs are periodically distributed in the asphalt overlay and stopped at the interface. Because only the deformation mismatch contributes to the tensile stress in the asphalt overlay, we can disregard the portion of uniform strain with the magnitude of overlay's strain. Therefore, only the mismatch deformation in the base layer is taken into account written in term of strain ε_x^0.

With the increase of the tensile strain in the base layer (the averaged strain denoted by ε_x^0), some uniformly distributed OMCs form across the thickness of the asphalt overlay. Based on the periodic boundary condition, one section marked by dot line box in Figure 2(a) is selected to represent all other sections. Plane strain problem will be considered for this fracture analysis (Anderson, 2005). When the tensile strain reaches a certain value, the marked section of the overlay with length 2λ will be cracked into two pieces. To solve the elastic field in the section at the moment just before the crack forms as seen in Figure 2(b), the superposition of a uniformly strained section in Figure 2(c) with the "reduced problem" in Figure 2(d) is employed. In Figure 2(d), the asphalt overlay is bonded to the base layer through a

frictional interface and subjected to a uniform compressive stress on its ends (Yin et al., 2008). Because the deformation of Figure2(c) is compatible between the asphalt overlay and the base layer, the strain field in the asphalt overlay is still uniform as ε_x^0 and no shear stress exists along the interface between the asphalt overlay and base layer. The stress in the asphalt overlay can be written as

$$\sigma_x^0 = E_1/(1-v_1^2)\varepsilon_x^0 \tag{1}$$

where the plane strain assumption is used (Anderson, 2005).

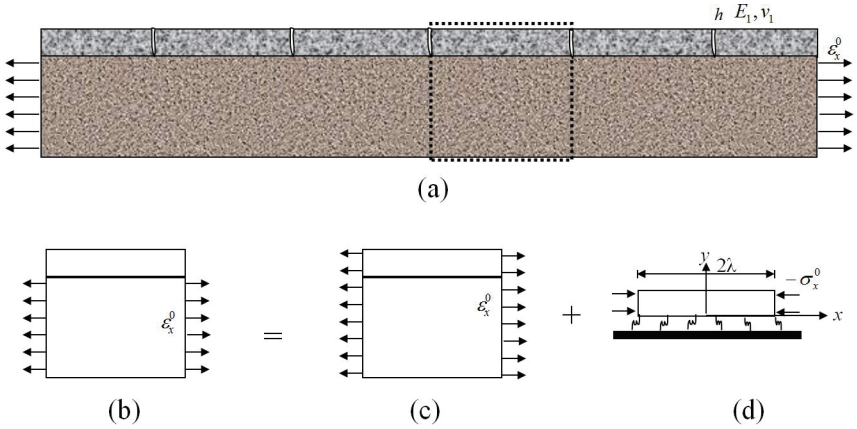

Figure 2. An asphalt overlay resting on a base layer with uniformly distributed discontinuities due to the mismatch deformation between two layers: (a) opening-mode crack map; (b) the marked section between two cracks; (c) the uniformly strained section, and; (d) the compressed section constrained by a frictional interface

To make the superposition of the problems in Figure 2(c) and 2(d) equivalent to the problem in Figure 2(b), in Figure 2(d) a uniform compressive stress $-\sigma_x^0$ is applied at the ends of the overlay, and the base layer is intact without other mechanical loading and provides constraint on the asphalt overlay through a frictional interface represented by springs. Superposition of the loadings in Figure 2(c) and 2(d) shows that the stress at the ends of asphalt overlay is zero, and the averaged strain in the base layer is ε_x^0. Therefore, the original problem is equivalent to the superposition of the two problems. Because the solution for the first problem in Figure 2(c) has been obtained in Equation (1), the original problem is reduced to the second problem in Figure 2(d).

To solve the reduced problem, a two dimensional (2D) Cartesian coordinate system is setup with the origin at the central bottom of the section with the section length 2λ. Notice that the effect of the stiffness and thickness of the base layer should be taken into account through the spring coefficient of the interface in Figure 2(d). In the literature, there exist several approaches to derive the spring coefficient from the geometry and material elastic properties of the two-layer system. Timm et al. (2003) proposed a benchmark model to derive the spring coefficient. The result is

independent on the material properties of the asphalt overlay but inversely proportional to the crack spacing. Xia and Hutchinson (2000) studied the OMCs in thin film/substrate systems and derived the spring coefficient based on the equivalence of energy release rate to the exact solution for an infinite long film containing one crack (Beuth, 1992). Suhir (1986, 1991) developed formulations for thim film/substrate systems with sparse and dense OMC patterns respectively. However, some issues about the derivation of the spring coefficient were brought forth (Basaran and Wen, 2006; Yin, 2009). Jain et al. (2007) proposed another form of spring coefficient based on the shear-lag model (Ji and Saruwatari, 1998). Yin et al. (2008) extended Xia and Hutchinson's (2000) method from 1D problem to 2D problem and provided more reasonable physical meanings. In asphalt pavement construction, the interface is typically treated with tackcoats, interlayers and other methods. Therefore, the spring coefficient may vary with specific conditions. It can be either experimentally measured or estimated from the above mentioned methods.

Because the thickness of asphalt overlay is much smaller than its length and the tensile load acts in the x direction with free surface, the top surface remains approximately flat for OMC if no debonding happens along the interface between the overlay and the base layer. Thus, it is assumed that all points of a plane normal to the y direction is still in the same plane after deformation (Yin, et al, 2008), i.e.,

$$u_y(x,y) = u_y(y). \tag{2}$$

Because no mechanical loading is considered in the vertical direction, we assume

$$\sigma_y(x,y) = 0. \tag{3}$$

Then the constitutive law reads

$$\sigma_x = \frac{E_1 u_{x,x}}{1 - v_1^2} \tag{4}$$

and

$$\tau_{xy} = \frac{E_1 u_{x,y}}{2(1 + v_1)}, \tag{5}$$

where $u_{y,x} = 0$ is used. The equilibrium equations in the absence of body force are written as:

$$\sigma_{x,x} + \tau_{yx,y} = 0, \tag{6}$$

i.e.

$$\frac{E_1}{1 - v_1^2} u_{x,xx} + \frac{E_1}{2(1 + v_1)} u_{x,yy} = 0. \tag{7}$$

By using the method of separation of variables, the general solution for the governing equation (7) can be obtained as

$$u_x = [A_1 sinh(cx/h) + A_2 cosh(cx/h)][B_1 sin(dy/h) + B_2 cos(dy/h)], \tag{8}$$

where $A_1, A_2, B_1,$ and B_2 are constants to be decided by the boundary conditions, x and y are normalized by the thickness h. In addition,

$$c = \sqrt{(1 - v_1)/2} \cdot d. \tag{9}$$

Because the surface of the overlay is free, the shear stress along the surface is zero, i.e.:

$$\tau_{yx}(x, h) = 0. \tag{10}$$

In addition, because the section is symmetric along y axis, the displacement satisfies

$$u_x(0, y) = 0. \tag{11}$$

Using the boundary conditions, we can simplify the solution in Equation (8) as

$$u_x = B sinh\left(c \cdot \frac{x}{h}\right) cos\left(d \cdot \frac{h - y}{h}\right). \tag{12}$$

Here are two independent parameters B and c or d to be determined by interface boundary condition and fractured surface boundary condition.

Along the interface, the compressive stress is transferred from the asphalt overlay to the intact base layer mainly through a shear stress. It is assumed that the displacement u_x is assumed to proportionally change with the shear stress τ_{yx} along the interface (Suhir, 1986; 1991; Xia and Hutchinson, 2000; Timm, et al., 2003; Jain, et al., 2007; Yin, et al., 2008) as:

$$\tau_{yx}(x, 0) = k u_x(x, 0), \tag{13}$$

where k is the spring coefficient that can be determined by experiments or estimated by the geometry and mechanical constants of the overlay and base layer materials. Notice that some researchers used the concept of interfacial compliance (Suhir, 1986; 1991; Yin, 2009), which is the reciprocal of the spring coefficient k.

The substitution of Equations (12) into (13) yields

$$d \cdot tan(d) = \frac{2(1+v_1)k}{E_1} h. \tag{14}$$

Here parameter d changes in the range of $0 - \pi/2$ and can be numerically solved from the above equation. Then, parameter c can be determined by Equation (9). When the right side term in Equation (14) is large, the solution of d will approach $\pi/2$. On the other hand, when it is small, $tan(d)$ can be approximated by d, and thus we can obtain:

$$d = \sqrt{\frac{2(1+v_1)k}{E_1} h} \text{ and } c = \sqrt{\frac{(1-{v_1}^2)k}{E_1} h}.$$

The above equation is applicable to thin lift of asphalt overlay an interlayer between the overlay and the base layer.

At the end of the asphalt overlay, the normal stress satisfies

$$\sigma_x(\lambda, y) = -E_1/(1-v_1^2)\varepsilon_x^0. \tag{15}$$

However, due to the assumption of Equation (2), the above boundary condition cannot be exactly satisfied. For simplicity, a weak form of the stress boundary condition is used, i.e. the resultant normal force being equivalent to the total stress, namely,

$$\int_{y=0}^{h} \sigma_x(\lambda, y) dy = -E_1/(1-v_1^2) \cdot h\varepsilon_x^0. \tag{16}$$

Substituting Equations (12) into (4) and then into (16), we can obtain

$$B = -\sqrt{\frac{2}{1-v_1}} \frac{h\varepsilon_x^0}{sin(d)\, cosh\left(\frac{c\lambda}{h}\right)}. \tag{17}$$

Therefore, a closed form elastic solution for the reduced problem is obtained. The superposition of the problems in Figure 2(c) and Figure 2(d) provides the solution for the original problem as

$$u_x = \left[x - \sqrt{\frac{2}{1-v_1}} \frac{sinh\left(c \cdot \frac{x}{h}\right) cos\left(d \cdot \frac{h-y}{h}\right)}{cosh\left(\frac{c\lambda}{h}\right) sin(d)} h \right] \varepsilon_x^0, \tag{18}$$

$$\sigma_x = \frac{E_1 \varepsilon_x^0}{1 - v_1^2}\left[1 - d\frac{cosh\left(c \cdot \frac{x}{h}\right) cos\left(d \cdot \frac{h-y}{h}\right)}{cosh\left(\frac{c\lambda}{h}\right) sin(d)}\right], \tag{19}$$

and

$$\tau_{yx} = -\frac{E_1 \varepsilon_x^0}{1 - v_1^2}\left[c\frac{sinh\left(c \cdot \frac{x}{h}\right) sin\left(d \cdot \frac{h-y}{h}\right)}{cosh\left(\frac{c\lambda}{h}\right) sin(d)}\right], \tag{20}$$

in which d and c are given in Equations (14) and (9).

3. Crack Initiation and Saturation

Consider the section with two OMCs at the both ends in Figure 2(b). When the external tensile loading increases to a critical value at ε_x^{cr}, a new OMC will nucleate along the central line. Just before the OMC initiates, the normal stress along the central line can be obtained from Equation (19) as

$$\sigma_x(0, y) = \frac{E_1 \varepsilon_x^{cr}}{1 - v_1^2}\left[1 - d\frac{cos\left(d \cdot \frac{h-y}{h}\right)}{cosh\left(\frac{c\lambda}{h}\right) sin(d)}\right], \tag{21}$$

and the shear stress is zero.

After a new OMC forms, the section is cracked into two pieces, and the elastic fields in each piece can also be solved by Equation (18) with replacing λ by $\lambda/2$ in the new local coordinate system. Then we can solve the crack opening displacement as

$$\delta(0, y) = 2\sqrt{\frac{2}{1 - v_1}}\frac{tanh\left(\frac{c\lambda}{2h}\right)}{sin(d)} cos\left(d \cdot \frac{h-y}{h}\right) h\varepsilon_x^{cr}. \tag{22}$$

To recover this crack opening displacement, the stress in Equation (22) has to be applied along the cracking surface. The energy released by this OMC is the work done by the stress in Equation (21) on the displacement in Equation (22) (Yin, et al., 2008). Thus, the energy release rate of the OMC can be written as

$$G = \frac{1}{2h}\int_{y=0}^{h} \sigma_x(0,y)\delta(0,y)\,dy. \tag{23}$$

By substituting Equations (21) and (22) into Equation (23), the energy release rate can be explicitly written as

$$G = \frac{E_1(\varepsilon_x^{cr})^2}{1-v_1^2}\frac{h}{c}tanh\left(\frac{c\lambda}{2h}\right)\left[1-\frac{d^2+d\cdot sin(d)cos(d)}{2cosh(c\lambda/h)sin^2(d)}\right]. \tag{24}$$

For different materials, the failure criterions can be fairly diverse. Fracture toughness has been widely accepted as a material constant and used for fracture analysis of asphalt pavements (Myers and Roque, 2002; Song, et al., 2006; 2008). Once the fracture toughness of the asphalt overlay is provided as Γ^{cr}, we can use it to determine whether any new fractures will be induced or not. If the energy release rate of the potential OMC is equal to or higher than the fracture toughness, the OMC will form. Therefore, the following criterion is used to predict the OMC spacing changing with the external loading:

$$\frac{E_1(\varepsilon_x^{cr})^2}{1-v_1^2}\frac{h}{c}tanh\left(\frac{c\lambda}{2h}\right)\left[1-\frac{d^2+d\cdot sin(d)cos(d)}{2cosh(c\lambda/h)sin^2(d)}\right] = \Gamma^{cr}. \tag{25}$$

When the mismatch strain ε_x^0 increases to ε_x^{cr} that is determined by the above equation, a new OMC will be induced to release the strain energy accumulated in the asphalt overlay. For an intact asphalt overlay, $\lambda/h \to \infty$, we obtain $cosh(c\lambda/h) \to \infty$ and $tanh(c\lambda/2/h) \to 1$. We can calculated the crack initiation condition as

$$\varepsilon_x^{cr} = \sqrt{\frac{c(1-v_1^2)}{E_1 h}\Gamma^{cr}}, \tag{26}$$

from which we can determine the tolerance of new constructed asphalt pavements for deformation mismatch between asphalt overlay and base layer. For low temperature cracking, if the temperature gradient is known in pavements, we can solve the deformation mismatch using the thermal expansion coefficient of the asphalt overlay and base layer. Therefore, the OMC initiation due to low temperature cracking can be predicted through Equation (26). Notice that the OMC initiation depends on the fracture toughness, Young's modulus, Poisson's ratio, and thickness of the asphalt overlay and the spring coefficient of the interface between the overlay and base layer.

In addition, with the increase of the crack density, the required deformation mismatch ε_x^{cr} to induce a new crack also increases as the following:

$$\varepsilon_x^{cr} = \sqrt{\frac{c(1-v_1^2)}{E_1 h \cdot tanh\left(\frac{c\lambda}{2h}\right)\left[1-\frac{d^2+d\cdot sin(d)cos(d)}{2cosh(c\lambda/h)sin^2(d)}\right]}\Gamma^{\mathrm{cr}}}. \tag{27}$$

In the above equation, when the crack spacing 2λ is reduced to a certain level, such as

$$1-\frac{d^2+d\cdot sin(d)cos(d)}{2cosh(c\lambda/h)sin^2(d)} = 0, \tag{28}$$

the required critical deformation mismatch ε_x^{cr} will be infinitely large. It means that no new OMC can initiate even for a large deformation mismatch. Therefore, crack saturation is observed. From Equation (28), the OMC saturation spacing, namely λ^s, can be obtained as

$$\lambda^s = acosh\left[\frac{d^2+d\cdot sin(d)cos(d)}{2sin^2(d)}\right]\frac{h}{c}. \tag{29}$$

When the OMC spacing approaches λ^s, even if the deformation mismatch is considerably large, the energy release rate at the central line of the section becomes small due to the last term in the Equation (24). Therefore, the potential for OMC is small. In addition, because the OMC is directly caused by the tensile stress in the asphalt overlay, Bai et al. (2000) used the stress transition from tensile to compressive at the middle point along the surface to determine the critical OMC saturation spacing. With extensive FEM simulation, they were able to determine λ^s changing with material constants and loading conditions. Using this criterion, we can also obtain λ^s from Equation (21) as:

$$\lambda^s = acosh\left[\frac{d}{sin(d)}\right]\frac{h}{c}. \tag{30}$$

The above equation provides a higher prediction of OMC saturation spacing than Equation (29) does. The reason is that when the stress at the center reaches a compressive status, a large range of stress distribution along the central line $x = 0$ still is in a tensile status, which makes the fracture energy release rate of the opening-mode fracture still high enough to drive a crack.

4. Numerical Results and Parametric Analysis

The proposed model is general and applicable to any deformation mismatch between asphalt overlay and base layer, which causes tensile stress in the overlay. However, the assumptions and/or approximations adopted may impose some limitations on the application of the formulation.

First, because the displacement in y direction is confined, all the points in the same plane perpendicular to y axis are assumed to keep in the same plane during deformation. Therefore, this assumption imposes a limitation of this model that the thickness and stiffness of the base layer should be large enough to provide the displacement constraint in y direction. For pavements with severe rutting distresses, the plane assumption may not be valid, so the accuracy of this model can be affected.

Secondly, to obtain an explicit, analytical solution for the governing equation, the boundary condition along the crack surface is approximated as a weak form boundary condition that the resultant force is equal to the total stress. This assumption aids to obtain a closed-form, simple solution without the loss of generality. However, it makes the stress field around the crack surface inaccurate. If needed, it can be justified by a series form solution (Yin et al, 2007).

Thirdly, the OMC development is limited within the asphalt overlay. The base layer is assumed to be intact and no delimination exists along the interface. When the crack penetrates into the base layer and the asphalt overlay debonds from the base layer, the cracking pattern will be changed, and some modifications have to be employed to use this model.

To show the capability of the proposed model, some numerical results and parametric analysis will be presented in the following parts.

Using Equations (19) and (20), the stress distribution in the asphalt overlay is investigated in the following three figures. Figure 3 illustrate the normal stress and shear stress distribution along the interface considering different spring coefficients of the interface. Here the length of the section is set at $\lambda/h = 5$. Because the Poisson's ratio will affect the parameter c and d, the Poisson's ratio for the asphalt overlay will be used as 0.35 in this paper (Song, et al., 2006; 2008). Both σ_x and τ_{yx} are normalized by $\sigma_x^0 = E_1\varepsilon_x^0/(1-v_1^2)$. Figure 3(a) showes that the normal stress along the interface reaches the maximum at the central point and decreases along with x axis for $x > 0$. When the spring coefficient is higher, the normal stress is larger because of the stiffer constraint for the deformation mismatch. It can be imagined that when the spring coefficient is extremely high, the constraint from the base layer can be considered as a rigid plate, so that the ratio of σ_x/σ_x^0 will keep at 1 for all the points along the interface. Figure 3(b) presents the normalized shear stress distribution. When the spring coefficient is higher, the shear stress is larger at the end of the section. However, it quickly reduces to zero at the center of the section. Notice that a stiffer interface may produce a lower shear stress in the middle range of the section.

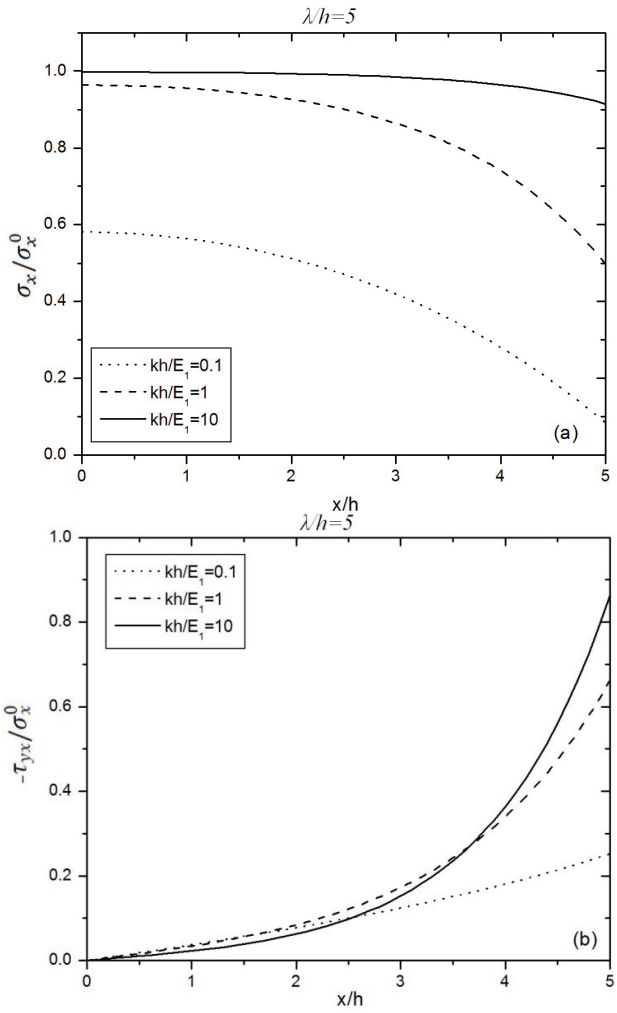

Figure 3. Stress distribution in asphalt overlay along the frictional interface between the overlay and base layer with different spring coefficients: (a) normal stress σ_x and (b) shear stress τ_{yx} normalized by $\sigma_x^0 = E_1\varepsilon_x^0/(1-\nu_1^2)$.

Figure 4 showes the normal stress and shear stress distribution along the interface of asphalt pavements for different crack spacing. Here the spring coefficient is set at $kh/E_1 = 1$. Three cases are studied as $\lambda/h = 1,2,\text{and } 5$. With the development of OMCs, the crack spacing is reduced. Both normal and shear stresses are considerably reduced due to the release of strain energy by the fracture. Figure 4(a) demonstrates the significant change of normal stress. Although at the ends of asphalt overlays, the normal stresses are similar for the three cases, the tensile stress at the center of the section, which is the driven force for a new crack, is

much lower for smaller crack spacing. Therefore, given a specific deformation mismatch, the crack spacing can be quantitatively determined, which will be demonstrated later. Figure 4(b) shows the distributions of shear stress. Because of the assumptions and approximations, the singularity of stress distribution cannot be exactly presented. However, Figure 4(b) still shows that shear stress is concentrated at the ends of section with a higher stress gradient for a longer section.

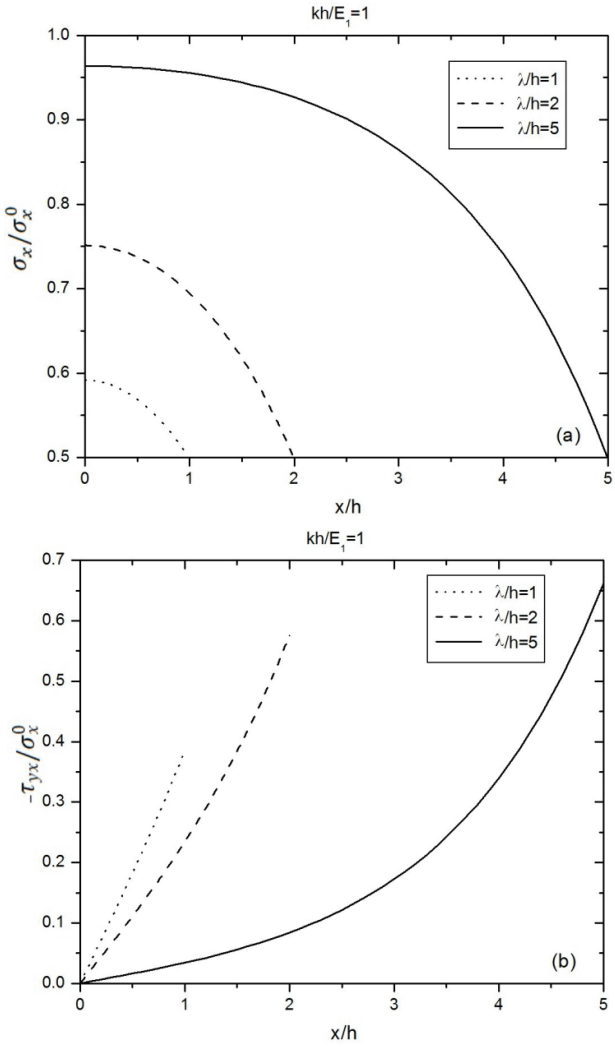

Figure 4. Stress distribution in asphalt overlay with different crack spacing: (a) normal stress σ_x and (b) shear stress τ_{yx} normalized by $\sigma_x^0 = E_1\varepsilon_x^0/(1-\nu_1^2)$.

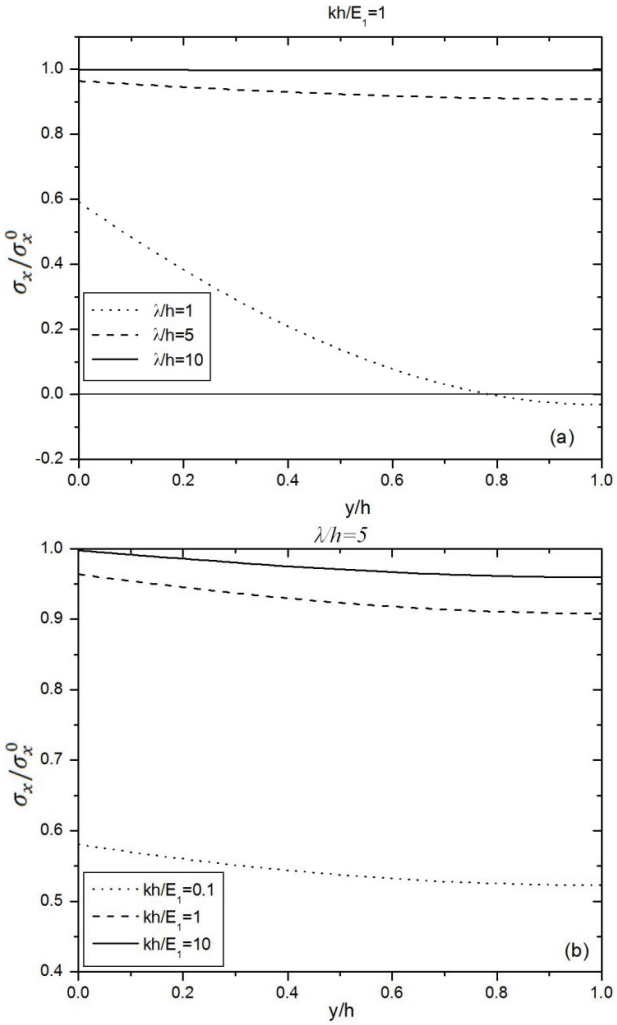

Figure 5. Distribution of normal stress σ_x along the central line of the section with (a) different crack spacing and (b) different spring coefficients of interface

Figure 5 provides the normal stress distribution along the central line of the section in the vertical direction. In Figure 5(a), when the crack spacing is larger such as $\lambda/h = 10$, the normal stress is almost constant in the thickness direction. When λ/h is smaller, the stress reduces and stress gradient in the thickness direction increases. When $\lambda/h = 1$, the normal stress considerably decreases from the bottom to the top of the overlay. Notice that the stress close to the surface is compressive although the resultant force cross the thickness is tensile. Figure 5(b) illustrates the

normal stress distribution in the asphalt overlay with different spring coefficients of interface. Here, $\lambda/h = 5$. Apparently, the higher the spring coefficient, the higher the normal stress. Therefore, a stiffer interface will produce higher tensile stress in the overlay for a certain deformation mismatch. However, it does not means that we should adopt compliant interface in the construction, because the energy release rate for a stiff interface may not be high due to the constraint of potential crack opening. In addition, interface debonding can be another concern if it is not handled with properly.

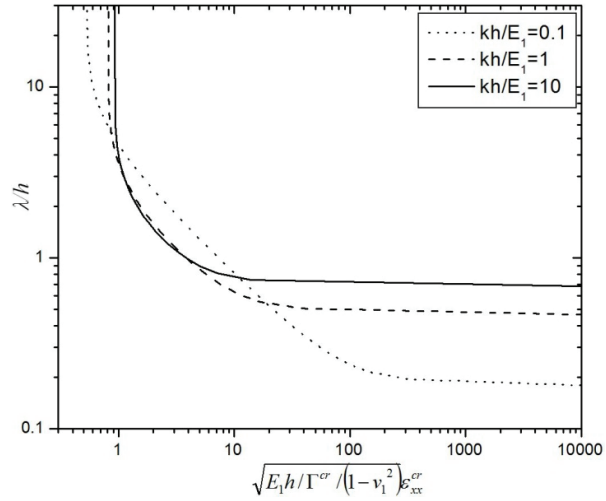

Figure 6. The OMC spacing development with the increase of the mismatch deformation between the asphalt overlay and the base layer

Using Equation (25), Figure 6 illustrates the crack spacing λ/h changing with a dimensionless parameter $\sqrt{E_1 h/\Gamma^{\mathrm{cr}}/(1-v_1^2)}\varepsilon_x^{cr}$, which represents the required tensile loading to form a new crack for a certain section with crack spacing λ. With the increase of the tensile loading, we can observe the following features:

- When the mismatch deformation is small, no fracture initiates even if λ/h approaches to the infinite. It means that for an intact asphalt pavement, *there exists a threshold of mismatch strain to induce the first OMC*, which can be calculated from Equation (26).
- When the external tensile loading increases to a certain value, the first OMC initiates. The stiffer the interface, the higher critical tensile strain to generate the first OMC. Therefore, *a stiffer interface provides advantages to control the OMC initiation.*
- Once the first crack is able to form, the crack spacing rapidly decreases with the external loading. Therefore, multiple OMCs may form within a small increase

of the loading. In field observation, *some OMCs may simultaneously form with fairly large crack spacing*.

- When the external tensile loading keeps increasing, more OMCs will be induced. The crack development in an asphalt pavement with a stiffer intact layer is much faster. When crack spacing λ/h is in the range between 1 to 3, the required external tensile loading for different types of pavements is very close. Therefore, *for a moderately dense crack pattern, strengthening the interface may not produce significant effect on the OMC resistance*.
- When the crack spacing is very small, the required tensile loading will be considerably large to produce a new OMC. When the fracture spacing reaches a certain level, no new OMC can be induced even when the tensile loading approaches the infinite. *The stiffer the interface between the overlay and the base layer, the larger the OMC saturation spacing*, which can be calculated from Equation (29).

5. Application and Discussion

To demonstrate the application of the proposed formulation, following we use some actual data of asphalt materials with different interfacial properties and analyzed the OMC behaviour under some loading conditions. The mechanical properties of asphalt overlay are as follows (Song, et al. 2006): $E_1 = 14.2GPa$, $v_1 = 0.35$, and $\Gamma^{cr} = 344J/m^2$.

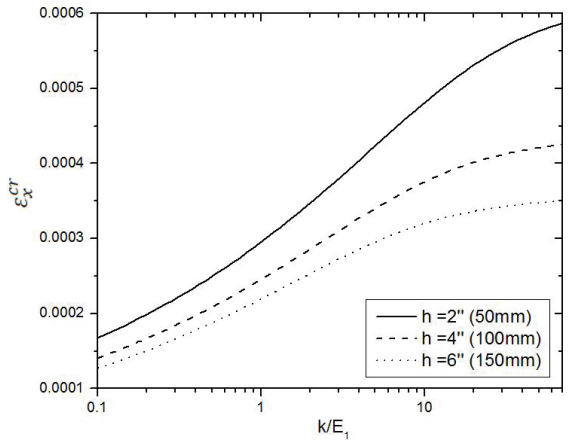

Figure 7. The critical mismatch deformation to cause the first OMC initiation changing with the spring coefficient of the frictional interface for asphalt overlays with different thicknesses

In pavement design, transportation engineers need provide the thickness of pavement layers based on asphalt materials and loading conditions. For a new constructed asphalt overlay with the above material constants, Equation (26) predicts the necessary mismatch deformation ε_x^{cr} to develop the first OMC. Figure 7 illustrates ε_x^{cr} changing with spring coefficients of the frictional interface for asphalt overlays with different thicknesses. Obviously, for a thinner overlay, a higher ε_x^{cr} is needed. With the increase of the spring coefficients of the frictional interface, ε_x^{cr} also increases. However, when the spring coefficient reaches a certain value, for example, $k/E_1 = 10m^{-1}$ for h=150mm, the interface can be approximated to be rigid, and ε_x^{cr} will not change too much with the increase of the spring coefficients.

Assume the asphalt overlay is subjected to a sudden temperature drop and OMCs are induced by low temperature cracking. Typically, the thermal expansion coefficient α_1 of asphalt materials is in the range of $1.3 - 3.0 \times 10^{-5}$ ℃$^{-1}$. Here let us say $\alpha_1 = 3.0 \times 10^{-5}$ ℃$^{-1}$. If the interface is compliant, the first OMC may form when the temperature difference between the asphalt overlay and the base layer reaches nearly 4, 5, 6 ℃ for h=150, 100, and 50 mm respectively. Therefore, *a thinner overlay even provides a better crack resistance performance for the first OMC initiation*. Common wisdom typically predicts that if a 50mm asphalt surface course lasts for 5 years, a 100mm asphalt surface course will last for around 10 years. Unfortunately, it does not work for OMC initiation. A thin overlay with a stiff interface provides the optimal performance for resisting OMC initiation. In this figure, a thin lift with $k/E_1 = 70m^{-1}$ for h=50mm can sustain a temperature mismatch of about 20℃ between the asphalt overlay and the base layer, which can represent some extreme cases in the field. From this relationship, transportation engineers can choose an appropriate overlay thickness of asphalt pavements for new construction or rehabilitation for resisting low temperature crack, considering the historic data of the local region.

Equation (26) is applicable for the first OMC in a long intact asphalt pavement. However, in many situations, transportation engineers need to analyze the OMC development for asphalt pavements with some cracks, such as reflective cracks and existing OMCs (Yin, et al., 2007). Equation (27) predicts the necessary mismatch deformation to induce a new OMC within a section of length 2λ. In Figure 8, we consider an asphalt pavement with a thin lift h=50mm. When λ/h is higher than a certain value λ^{cr}, ε_x^{cr} changing with λ/h is very small. Therefore, once the first OMC initiates, crack spacing will be quickly reduced to λ^s. With the decrease of the crack spacing, the driven force to cause a new crack will be much higher. When λ/h is reduced to another certain value λ^s, no matter how large the mismatch deformation is, no new cracks can initiate.

For example, for a stiff interface with $k/E_1 = 100m^{-1}$, once ε_x^{cr} increases to around 0.0006, OMCs start, and the crack spacing will be quickly reduced to

$2\lambda = 0.4m$ or $\lambda/h = 4$. With the increase of the mismatch deformation, crack spacing will be saturated at $2\lambda = 0.1m$ or $\lambda/h = 1$. Therefore, OMC crack spacing essentially changes in the range of 0.1 – 0.4 m for this thin lift with a very stiff interface. However, for a compliant interface, the crack spacing may change in a much bigger range. Notice that although asphalt pavements with a stiffer interface exhibit better resistance for the first OMC initiation and larger saturation crack spacing, *it does not mean that a stiffer interface always presents a larger crack spacing for any given mismatch deformation*. For example, for asphalt pavements with $k/E_1 = 100, 10, 1,$ and $0.1m^{-1}$ under $\varepsilon_x^{cr} = 0.002$, the crack spacing λ/h will be 1.1, 1.3, 2.2, and 4.6, respectively.

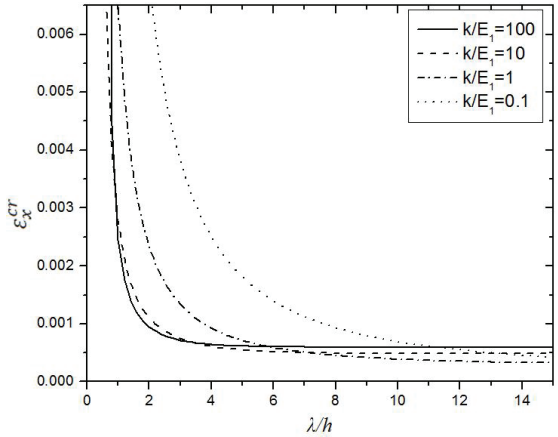

Figure 8. The critical mismatch deformation to cause a new OMC initiation for an asphalt overlay with changing section length for different spring coefficients of the frictional interface (h=50mm)

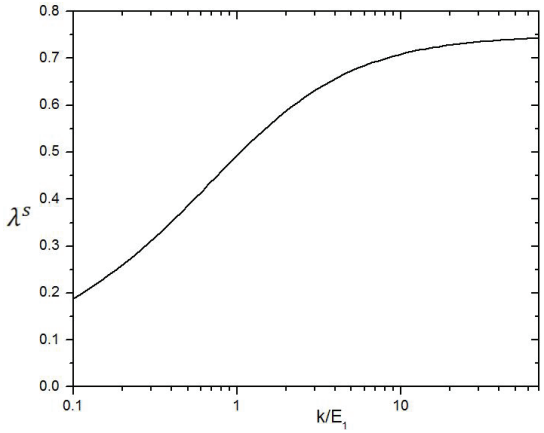

Figure 9. The OMC saturation spacing of asphalt pavements changing with the spring coefficient of the frictional interface

Equation (29) provides the theoretical OMC saturation spacing λ^s. Figure 9 shows λ^s changing with the spring coefficient of the frictional interface. With the increase of k/E_1, λ^s also increases. However, when $k/E_1 > 20m^{-1}$, the change of λ^s will not be significant.

Notice that the formulation in this paper is developed based linear elastic assumption. However, asphalt materials exhibit viscoelastic behaviour in a large temperature range. At low temperatures, if OMCs are developed transiently, the proposed formulation can be directly used because the viscoelastic behaviour only produces minimum effects on OMC development. However, if OMCs form over a certain period, some strain energy will be dissipated through the creep behaviour, therefore, fewer OMCs are needed to release the stored strain energy. Therefore, the actual crack spacing and the required mismatch deformation can be much larger than the present results. An extension of this work from elastic modelling to viscoelastic modelling is underway. On the other hand, due to the defects or material variation in asphalt pavement construction, in field OMCs may exhibit in the mixed-mode and the crack pattern may be non-uniform. However, statistically, OMCs can be recognized through the averaged crack spacing and the corresponding mechanical loading condition.

In addition, the spring coefficient of the frictional interface is still needed to be quantitatively characterized. Although some models have been existed in the literature, the accuracy and applicability are to be validated in the future. It will be of great significance if an experimental approach can be developed to directly measure it.

6. Conclusions

Opening-mode cracking in asphalt pavements is studied and a two-dimensional closed-form elastic solution of one section from the periodic crack pattern is derived. Using the fracture energy criterion, the proposed model predicts the OMC initiation and saturation. The OMC development with mismatch deformation can also be simulated. Given a loading condition, a critical thickness of the asphalt overlay, below which no OMC can be induced, can be determined. The explicit formulation can be conveniently used in pavement design and failure analysis. Based on the simulation and analysis, some interesting findings are summarized as follows:

- For an intact asphalt pavement, there exists a threshold of mismatch deformation to induce the first OMC. The stiffer the interface, the higher the threshold mismatch deformation.
- Once the first crack forms, the crack spacing rapidly decreases to a certain value λ^{cr}. Therefore, multiple OMCs may simultaneously form. The stiffer the interface, the lower the crack spacing λ^{cr}.
- When crack spacing approaches a certain value λ^{s}, the driven force to produce a new OMC will be significantly high. If crack spacing is less than λ^{s}, no new OMC can be induced. λ^{s} is proportional to the thickness of the overlay.
- OMC crack spacing changes from λ^{cr} to λ^{s}. An asphalt pavement with a stiff interface has a narrow crack spacing range.
- Given asphalt material properties and loading condition, there exists a critical thickness for the asphalt overlay, below which no OMC can initiate. Therefore, a thinner asphalt overlay may produce better performance for OMCs.

Because asphalt materials exhibit viscoelastic behaviour, the present elastic formulation may overly predict the OMC crack density. Future work to quantitatively evaluate the effect of the assumptions and release those assumptions is underway.

Acknowledgements/disclaimer

The author acknowledges the financial support from the University Transportation Research Center (UTRC). The results and opinions presented herein are those of the author and do not necessarily reflect those of the sponsoring agency. The author is also grateful for the help of Professor W.G. Buttlar and Dr. E. Dave for taking the photos of asphalt pavements. In addition, the author would like to thank Professors G.H. Paulino and W.G. Buttlar for their comments on fracture analysis.

7. References

Anderson, T. (2005). *Fracture Mechanics: Fundamentals and Applications* (3rd Ed ed.). CRC.

Bai, T., Pollard, D., & Gao, H. (2000). Explanation for fracture spacing in layered materials. *Nature , 403*, 753-756.

Basaran, C., & Wen, Y. (2006). Influence of Interfacial Compliance on Thermomechanical Stresses in Multilayered Microelectronic Packaging. *IEEE Transaction of Advanced Packaging , 29*, 666-673.

Beuth, J. (1992). Cracking of thin bonded films in residual tension. *International Journal of Solids and Structures , 29*, 1657-1675.

Harmelink, D., Shuler, S., & Aschenbrener, T. (2008). Top-down cracking in asphalt pavements: causes, effects and cures. *Journal of Transportation Engineering, ASCE , 134*, 1-6.

Huang, Y. (2003). *Pavement analysis and design.* Englewood Cliffs, NJ: Prentice-Hall.

Jain, A., Guzina, B., & Voller, V. (2007). Effects of overburden on joint spacing in layered rocks. *Journal of Structural Geology , 29*, 288-297.

Ji, S., & Saruwatari, K. (1998). A revised model for the relationship between joint spacing and layer thickness. *Journal of Structural Geology , 20*, 1495-1508.

Kim, H., & Buttlar, W.G. (2009). Discrete Fracture Modeling of Asphalt Concrete, *International Journal of Solids and Structures*, 46(13), 2593-2604.

Kim, H., Wagoner, M.P., & Buttlar, W.G. (2009). Micromechanical Fracture Modeling of Asphalt Concrete Using a Single-Edge Notched Beam Test, *Materials and Structures*, 42(5), 677-689.

Luo, Z., & Yin, H. (2008). Probabilistic Analysis of Pavement Distress Ratings with the Clusterwise Regression Method. *Transportation Research Board , 2084*, 38-46.

Myers, L., & Roque, R. (2002). Top-Down Crack Propagation in Bituminous Pavements and Implications for Pavement Management. *Journal of the Association of Asphalt Paving Technologists , 71*.

Song, S., Paulino, G., & Buttlar, W. (2006). Simulation of crack propagation in asphalt concrete using an intrinsic cohesive zone model. *Journal of Engineering Mechanics-ASCE , 132*, 1215-1223.

Song, S., Wagoner, M., Paulino, G., & Buttlar, W. (2008). delta(25) Crack opening displacement parameter in cohesive zone models: experiments and simulations in asphalt concrete. *Fatigue & Fracture of Engineering Materials & Structures , 31*, 850-856.

Suhir, E. (1986). Interfacial stresses in bimetal thermostats. *Journal of Applied Mechanics - ASME , 53*, 657-660.

Suhir, E. (1991). *Structural Analysis in Microelectronic and Fiber-Optic Systems.* New York: van Nostrand Reinhold.

Timm, D., Guzina, B., & Voller, V. (2003). Prediction of thermal cracking. *International Journal of Solids and Structures , 40*, 125-142.

Wang, L., Myers, L., Mohammad, L., & Fu, Y. (2003). Micromechanics Study on Top-Down Cracking. *Transportation Research Record , 1853*, 121-133.

Xia, Z., & Hutchinson, J. (2000). Crack patterns in thin films. *Journal of the Mechanics and Physics of Solids , 48*, 1107-1131.

Yin, H. (2009). Comment on "Influence of Interfacial Compliance on Thermomechanical Stresses in Multilayered Microelectronic Packaging" (IEEE Trans. Adv. Packaging, 29, 666-673, 2006). *IEEE Transaction of Advanced Packaging*, (in press).

Yin, H., Buttlar, W., & Paulino, G. (2005). A two-dimensional elastic model of pavements with thermal failure discontinuities. *3rd MIT Conference on Computational Fluid and Solid Mechanics*, (pp. 539-542). Boston.

Yin, H., Buttlar, W., & Paulino, G. (2007). Simplified Solution for Periodic Thermal Discontinuities in Asphalt Overlays Bonded to Rigid Pavements. *Journal of Transportation Engineering, ASCE , 133*, 39-46.

Yin, H., Paulino, G., & Buttlar, W. (2008). An explicit elastic solution for a brittle film with periodic crack. *International Journal of Fracture , 153*, 39-52.